HHS Public Access

Author manuscript

Trans Soc Min Metall Explor Inc. Author manuscript; available in PMC 2019 May 01.

Published in final edited form as:

Trans Soc Min Metall Explor Inc. 2018 January ; 344(1): 31–37. doi:10.19150/trans.8746.

Analysis of extensometer, photogrammetry and laser scanning monitoring techniques for measuring floor heave in an underground limestone mine

B.A. Slaker and **M.M. Murphy**

Mining engineer and mining engineer, respectively, National Institute for Occupational Safety and Health, Pittsburgh, PA, USA

T. Miller

Geologist, East Fairfield Coal Company, Lima, OH, USA

Abstract

An underground limestone mine in eastern Ohio was experiencing significant floor heave and roof falls, attributed to high horizontal stresses. Areas of the mine showing floor heave were monitored with roof-to-floor extensometers and photogrammetry surveys to determine the rate and magnitude of heave. Extensometer data were recorded hourly at four locations across adjacent entries while photogrammetry surveys of the floor were performed at the same locations every two to five weeks. A final survey was performed using an I-Site 8200 laser scanner. Following instrumentation, floor heave up to 10.1 cm (4 in.) was measured by the extensometers, photogrammetric reconstructions and laser scanner over a six-month period. The extensometers were biased by the location where they were placed, failing to consistently capture the location and extent of floor heave and cracking. The photogrammetry surveys were not precise enough to capture small magnitude movements. Mining in the area was halted and within several months the floor movement and incidence of roof falls were significantly lessened.

Keywords

Limestone; Underground mining; Photogrammetry

Introduction

Limestone formations in the United States can be subject to relatively high horizontal stresses due to the presence of tectonic loading of the strata. Horizontal stresses have a documented history of causing stability issues in underground limestone mines. Kuhnhein and Ramer (2004) discussed the influence of horizontal stress on complex ground control interactions associated with limestone pillar design and mine layouts. Esterhuizen, Dolinar and Iannacchione (2008) documented roof damage observations associated with high

horizontal stresses such as roof guttering, beam instability, oval-shaped falls and failure propagations. There have also been a number of documented case histories of horizontal stress causing unexpected roof and pillar failures at shallow depths (Stacey and Yathavan, 2003). To our knowledge, there has only been one well-documented case of floor failure causing stability issues in an underground limestone mine. Murphy et al. (2015) documented the role of a weak, moisture-sensitive floor in the development of a massive roof collapse.

For the present paper, the study site neighbored the site in Murphy et al. (2015) and had the same general geology. However, the weak, moisture-sensitive floor was not present for the current study. The current study site has experienced significant floor instabilities caused by high horizontal stresses. The instability area was monitored using two different methods to determine if the floor failure would eventually propagate into roof or pillar failure. The objective of this paper is to analyze displacement monitoring measurements from string potentiometers and two wide-area point capture techniques in an area experiencing active movement. Based on the measurement trends and observed damage from inside of the mine, the presumed failure process will be discussed.

The study site is the Subtropolis Mine, an underground limestone operation located near Petersburg, OH, and owned by East Fairfield Coal Company. The surface terrain is relatively flat and mining depths range from 38 to 55 m (125 to 180 ft). The mine is situated in the Vanport Limestone, part of the Allegheny Formation within the Pennsylvanian System. At the study area, the pillars were 15 m (50 ft) long by 9 m (30 ft) wide. The mining height was approximately 5.5 m (18 ft), leaving a planned 1.2-m (4-ft) beam of limestone in the immediate roof. The limestone beam was inconsistent in some areas, having a thickness as low as 0.6 m (2 ft). Above the roof limestone beam was mostly weak shale extending to the surface. However, approximately 9 to 12 m (30 to 40 ft) above the limestone resided the Lower Kittanning coal seam. Strength testing was conducted from a neighboring mine which reported shale roof uniaxial compressive strength ranging from 53 to 75 MPa (7,660 to 10,750 psi). The limestone roof beam and limestone pillar had strength ranging from 93.5 to 120 MPa (13,570 to 17,880 psi). These results were assumed to be similar to the current study site due to the close proximity between mines.

Directly below the pillar was a 0.9-m (3-ft) beam of floor limestone that was observed to be geologically different roof and pillar limestone since it was naturally blockier and not intact. Although no strength testing was available for the floor limestone, it was presumed to be stiffer than the roof and pillar limestone due to other research performed in the same geographical area (Murphy et al., 2015). Beneath the floor limestone was a thick sandstone bed.

Previous research conducted at the mine also revealed high horizontal stresses, indicated by cutter roof failures and the observation of significant movement in test holes (Ellenberger and Miller, 2012). The same movement in the test holes was witnessed during this study by the mine geologist. Additionally, the presence of significant floor heave with a competent limestone floor unit and minimal pillar condition change suggests that the heave was not due to pillar punching but rather a horizontal stress transfer. The high horizontal stress has

resulted in the weakening of both the roof and floor limestone, causing floor heave and roof collapse.

The roof collapses near the studied area began to occur in entry 2 (Fig. 1) on Feb. 24, 2016. It then moved to entry 1, followed by entry 3 and then entry 4, progressing through all four in less than a month. The crosscut floor in the collapsed zone between entries 5 and 6 was observed to have heaved an estimated 15.2 to 25.4 cm (6 to 10 in.) several days prior to failure of the roof. The failures, visible in Fig. 2, eventually extended upward to the overlying Lower Kittanning coal seam.

In addition to the roof collapses, observable floor heave, shown in Fig. 3, was present near the unstable sections of the mine. This floor heave was of particular interest because it was the most visible manifestation of the horizontal stress before roof failure renders an area inaccessible. Previous research by the U.S. National Institute for Occupational Safety and Health (NIOSH) found the maximum horizontal stress to be in the N-S direction (Ellenberger and Miller, 2012), rather than the N50–80°E direction indicated by the World Stress Map (Mark and Gadde, 2008; Zoback and Zoback, 1989).

Methods

The instrumentation consisted of four roof-to-floor string potentiometers, hereafter referred to as extensometers, installed near four separate intersections following the N35°E trending roof collapses, shown in Fig. 1. The extensometers were anchored to roof bolt plates using a strong magnet and anchored to the floor by a weighted metal plate. Each extensometer was wired into a MIDAS data logger (Jones, 2012) where a measurement was recorded once every hour. Extensometers #1 and #2 were proactively placed in intersections that had no visible cracking, but were expected to heave if the failures progressed. Extensometers #3 and #4 were placed approximately 6.1 m (20 ft) and 15.2 m (50 ft), respectively, outby the first observed cracks, anticipating the heave would progress down the entry. An example of the extensometer placement with a nearby floor crack is shown in Fig. 4. An orange spray paint was initially used to mark visible floor cracks, and as the cracking progressed, the extensometers were placed near the cracks that appeared to show the most movement.

In addition to the extensometers, photogrammetry surveys were performed at each of the four instrumented locations during data collection visits between April 1 and Aug. 3, 2016. These surveys focused on the area surrounding the extensometers because those areas exhibited the most floor heave and thus would provide a reliable calibration point to compare movement measured by the photogrammetry to movement measured by the extensometers. For the photogrammetry surveys, a Nikon D5500 DSLR camera was used with an AF-S NIKKOR 20-mm f/1.8G lens and an auxiliary Metz 76 MZ-5 flash. Agisoft Photoscan (Agisoft LLC, 2015) was used for photogrammetric reconstruction and initial referencing while CloudCompare was used for distance measurements and fine point cloud alignment.

Between 200 and 250 photographs were taken during each visit, across the four extensometer locations. An example of the photograph locations is given in Fig. 5. The

photographs were angled toward the base of the pillar, ensuring that the floor was captured as well as the pillar, which would be used as an assumed stationary reference. The entire survey typically required about 1.5 to 2.5 h to perform. Although the objective of the study was to monitor floor movement, it was found during the course of the study that the floor made a poor subject for photogrammetry for several reasons:

- Ensuring adequate and consistent lighting across large areas of floor was difficult with the flash lighting.
- There was very little contrast or changing features in the floor, making point and pattern identification difficult.
- The small aperture size necessary to capture the high depth of field that comes with large areas of floor creates exposure concerns in the dark underground mine environment.
- False rock movements can appear due to fallen roof or rib material or the perturbation of the ground due to personnel or vehicle traffic.

To account for many of these difficulties, a set of photographs was collected in close proximity to each extensometer with a high angle of incidence with the floor. These closer photographs provided a high-resolution, consistently lit view of the extensometer and scale, and are responsible for the bulk of the reconstructed floor models.

For the last visit to the mine, on Oct. 13, 2016, a Maptek I-Site 8200 laser scanner was used to obtain the mine geometry. To maintain consistency, these scans were scaled and referenced to the April 1 photograph sets, instead of using the precise distances measured by the scanner or its own local coordinate system. The scale in the laser scanning is likely more accurate than the photogrammetry, but the size reduction required to make the laser-scanned point cloud match the photogrammetry point clouds was less than 1 percent, suggesting that the scale for the photogrammetry point clouds was acceptable. The assumption was made that the pillars could be trusted as a stationary reference in both of the wide-area point capture methods, with the exception of small-scale spalling.

Results and discussion

Throughout the April 1 to Oct. 13, 2016, study period, very little change in the floor or movement in the roof around the four study areas was visible to the naked eye. However, roof, floor, and pillar failure observations during this time include:

- Minor progression of the collapsed zone in the extensometer #3 and #4 entries toward the instruments.
- Consistent and audible roof failure two entries west of extensometer #1 on April 28.
- Signs of spalling or cracking in the southwest corner of the pillars near the study area.

- Development of a crack near extensometer #3 where one side lifted up away from the other, creating a roughly 2.5-cm (1-in.) vertical difference between the sides.

The precise amount of movement occurring in mine openings before the extensometers were installed is unknown, but it was sufficiently visible to prompt the mine personnel to install extensometers at the location. In order to create floor cracks of the size seen at the study sites, most likely a floor heave between 2.5 and 7.6 cm (1 and 3 in.) had occurred at the worst locations prior to instrumentation. The failure of the floor due to horizontal stress, and subsequent stress redistribution, is believed to be the cause of the ground stability issues.

In response to the heave, exploratory holes were excavated in the floor using a backhoe at the extensometer #3 location. At this location the floor consisted of a stiffer, and more impure, silica-rich limestone approximately 61 to 76 cm (2 to 2.5 ft) thick, underlain by a sandstone. The limestone in the floor consisted of thinner beds interbedded with thicker massive beds. The top 28 cm (11 in.) of the limestone in the floor, where it was more thinly bedded, was broken and could be excavated with ease, while the bottom of the limestone appeared solid. The solid, massively bedded limestone may have been bent or broken, but it was not shredded in the same way as the thinly bedded limestone. The floor was showing clear signs of vertical movement, but there was no visible evidence that roof movement was occurring at the four study sites, such as fallen rocks or cracking. Audible roof cracking in the failed areas was still occurring, but this did not appear to extend into the study area. As a result, the study progressed with photogrammetry being used to monitor floor heave, ignoring the roof as a potential source of movement.

Beginning with the photogrammetric measurements, the reconstruction for the floor surrounding extensometer #1 is shown in Fig. 6. The reconstructions represent the difference in vertical displacement between April 1 and the listed dates. Displacement upward toward the roof is shown in warmer colors while displacement downward into the floor is shown in cooler colors. A N45°E trending heave clearly developed near the middle of the intersection, away from where the extensometer is located. The extensometer would have missed this heave development without the photogrammetry.

Very little appears to be occurring in the reconstructions of the extensometer #2 site, shown in Fig. 7. This is the area that shows the least movement among the extensometers, and the photogrammetry supports that inactivity. There does appear to be a small magnitude widespread heave movement through May 25 followed by a sinking movement through Aug. 3. The manner of widespread displacement without an apex that would be expected with floor heave could suggest a reconstruction, scaling, or alignment error.

The extensometer #3 site had a large, visually distinct crack development slightly northwest of the extensometer on the east side of the intersection, which can be observed in the photogrammetric reconstruction, shown in Fig. 8. Oddly, the crack itself runs N75°W while the heave is oriented in a N25°W direction. Interestingly, the direction of the heave is offset by approximately 50° to the crack orientation, which was not immediately apparent upon visual inspection of the crack underground. While the large crack was present throughout each of the data collection visits, the N75°W heave did not begin until sometime after the

April 14 visit. The intersection immediately north of the extensometer was clear enough to walk through on March 18. However, progressive failure of the roof had completely sealed off the intersection by April 28. Additionally, southwest of the extensometer, an area approximately 4.6 m (15 ft) long, running parallel to the base of the pillar, was heaving upward.

The last site, the extensometer #4 location, shown in Fig. 9, exhibited the most floor heave. Due to the high magnitude and exclusively heaving behavior, the scale has been changed to represent absolute difference rather than signed change. A large area oriented N10°E, roughly 6.1 m (20 ft) across and more than 9.1 m (30 ft) long, was heaving in between two pillars, north of the intersection. The extensometer was very fortunately placed near the apex of the heave, capturing the largest magnitude movements.

The roof-to-floor extensometers showed varying magnitudes of displacement, but all showed a convergence of the mine openings. Figure 10 compares the extensometer measurements to the photogrammetry and laser scanning displacement measured at the same location. The first half of the monitoring period showed the most movement for all the extensometers, with rates reaching as high as 0.15 cm/d (0.06 in./d) for extensometer #4 during April. By late May, the rate of convergence had significantly lessened and the frequency of roof falls in the vicinity subsided.

The largest increase seen during the study period was 11 cm for extensometer #4 between March 1 and Aug. 25, as read by the extensometer. This was tracked very closely by the photogrammetry measurements, which underestimated the heave by 0.2 to 0.5 cm on each reading. The laser scan for this area showed nearly 7 cm of heave between April 1 and Oct. 13. Extensometer #3 showed a slight jump on March 24, followed by unevenness for the remainder of the monitoring period. This extensometer was located on top of two cracks, which were present before March 24, and is nearby several others. The reason for this is unknown. However, this area appears to have consisted of an intact floor beam several inches thick, underlain by about 20.3 cm (8 in.) of crushed rock. It may be that the beam buckled somewhere nearby the extensometer on March 24, and the noisy movement is related to the crushed rock pushing up on the compromised beam, with the beam then settling back down on the crushed rock.

Comparison of extensometer to photogrammetry results

The photogrammetry results agree very well with extensometer #4, shown in Fig. 10, but does not show the same increase in vertical displacement seen at the other extensometer locations. The magnitude of displacement seen in extensometers #1 to #3 is very small, although generally positive across all of them. The magnitude of displacement seen in the photogrammetry, however, had time periods of negative change. This is mostly seen at locations #2 and #3, which would suggest the floor was sinking slightly from its April 1 position. A rock fall compromised the cable for extensometer #4 in late August, and any data after that event were discarded. There were five photogrammetry data sets collected throughout the course of the study. Set equal to the extensometer data on April 1, each photogrammetry convergence measurement is calculated by averaging the elevation of the

points in a small area surrounding the extensometer. These areas were reduced to an approximately equal point cloud density to mitigate the effects of uneven densities when the elevation changes from one side of the extensometer to the other.

The photogrammetry results either point to the precision of the process being inadequate at these magnitudes of floor heave, or a combination of floor heave and roof sag may have occurred, which would not have been captured in the photogrammetry because the roof was not photographed. The laser scanning results, represented by a point measurement on Oct. 13 in Fig. 10, when compared to the first photogrammetry set, are much closer to the measured extensometer value. However, the laser scanning measurement still only capture about 80 to 85 percent of the total heave experienced by the extensometers. It may be that the initial April 1 photogrammetry survey, to which everything was compared, underestimated the floor heave by about 0.5 cm, and this bias carried throughout the experiment. The surveys at the extensometers #1 to 3 locations would suggest that the error associated with this photogrammetry process is significant compared to the magnitude of movement being measured.

The potential precision of photogrammetry has been well-documented. However, the method for employing the technique at this site produced imprecise heave magnitudes. More photographs of ribs and the connection between the ribs and floor would have improved registration accuracy. The general shape and location of heave seems to be accurate, and was validated with observations made underground. The ability to identify multiple areas of movement or describe the shape of the heave is not feasible with point measurement devices, and this is where wide-area point capture methods excel.

Conclusion

The Subtropolis underground limestone mine in Eastern Ohio was experiencing significant horizontal stress-induced ground failures. These failures included significant floor heave followed by roof collapse. Monitoring floor heave can be difficult with point measurements and visual observational methods are unreliable. Therefore, photogrammetry and laser scanning methods were used in addition to point measurements to assess the magnitude and location of floor heave.

Extensometers showed convergence of the opening ranging from approximately 1.3 cm (0.5 in.) at extensometer #2 to nearly 11.4 cm (4.5 in.) at extensometer #4. Most movement occurred in the first few months of the study period, and an unknown but significant amount of heave occurred before instruments were installed. The reduced rate of convergence follows the cessation of mining in that region.

The photogrammetric methods employed were reliable in assessing the location and shape of floor heave, but were too imprecise to match the extensometer performance of monitoring very small movements. Only the extensometer #4 location showed comparable results on both the photogrammetry and the extensometer. Several locations were identified through the photogrammetry that showed heave behavior not detected with the extensometers. The laser scanning survey, while only conducted on the last visit, rather than in a time-lapse

manner, is likely the most ideal method for monitoring floor heave, where it is not cost-prohibitive. Considering the experience in this case study, point measurements are insufficient to capture the extent of floor heave, and the failure of a single instrument or localized movement can result in misleading or incomplete interpretations of ground movement.

References

AgiSoft LLC, 2015, "Agisoft PhotoScan Professional Edition (Version 1.2.3)," retrieved from www.agisoft.com.

Ellenberger J, and Miller T, 2012, "Mitigating the effects of high horizontal stress on ground control in an underground stone mine: A case history," 31st International Conference on Ground Control in Mining.

Esterhuizen GS, Dolinar DR, and Iannacchione AT, 2008, "Field observations and numerical studies of horizontal stress effects on roof stability in US limestone mines," Journal of the South African Institute of Mining and Metallurgy, Vol. 108, No. 6, pp. 345–352.

Jones T, 2012, "Knowledge is power: Introducing the Midas, a new permissible datalogging system for use in mines," 31st International Conference Ground Control in Mining.

Kuhnhein G, and Ramer R, 2004, "The influence of horizontal stress on pillar design and mine layout at two underground limestone mines," Proceedings of the 23rd International Conference on Ground Control in Mining.

Mark C, and Gadde M, 2008, "Global trends in coal mine horizontal stress measurements," 27th International Conference Ground Control in Mining, pp. 319–331.

Murphy MM, Ellenberger JL, Esterhuizen GS, and Miller T, 2015, "Roof and pillar failure associated with weak floor at a limestone mine," Transactions of the Society for Mining, Metallurgy & Exploration, Vol. 338, pp. 502–509.

Stacey TR, and Yathavan K, 2003, "Examples of fracturing of rock at very low stress levels," 10th ISRM Congress.

Zoback ML, and Zoback MD, 1989, "Tectonic stress field of the continental United States," Geological Society of America Memoirs, Vol. 172, pp. 523–540, 10.1130/mem172-p523.

Figure 1 -

Extensometer locations, shown as blue stars, along with crack locations and orientations, shown as red lines, and the dates they were first observed.

Figure 2 -
Roof collapse area.

Figure 3 -
Floor buckling.

Figure 4 -
Extensometer #3 located near a previously observed floor crack.

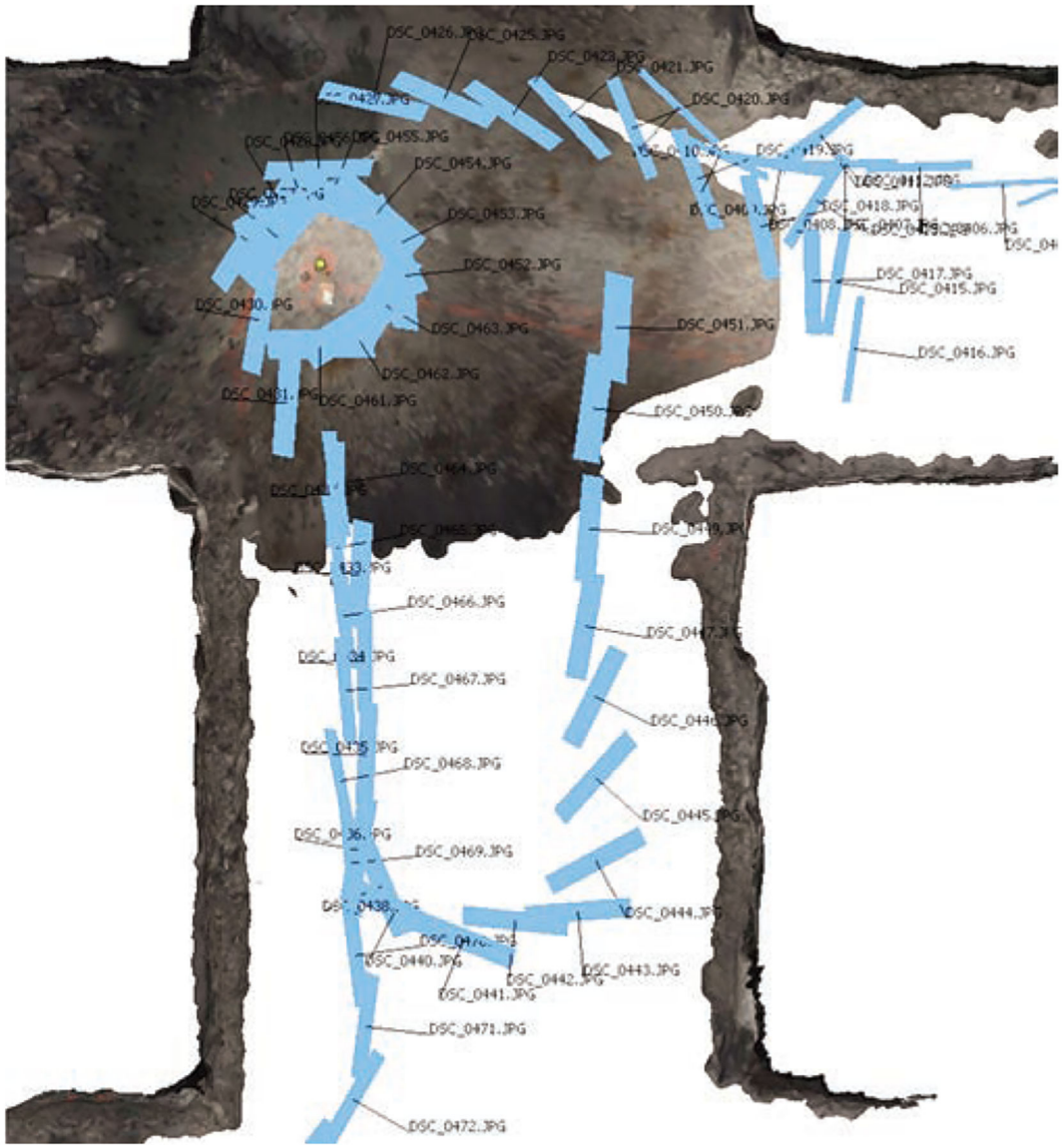

Figure 5 -
Photograph locations and photogrammetric reconstruction at the extensometer #2 site.

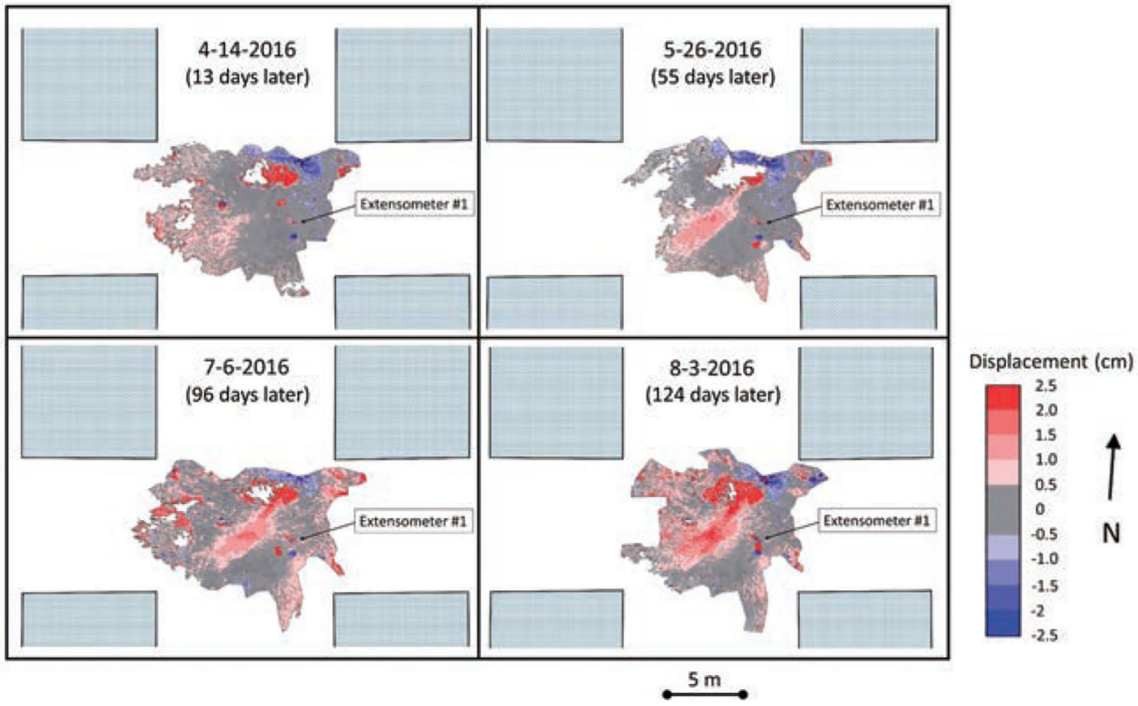

Figure 6 -

Floor movement according to the photogrammetric reconstruction at the extensometer #1 location.

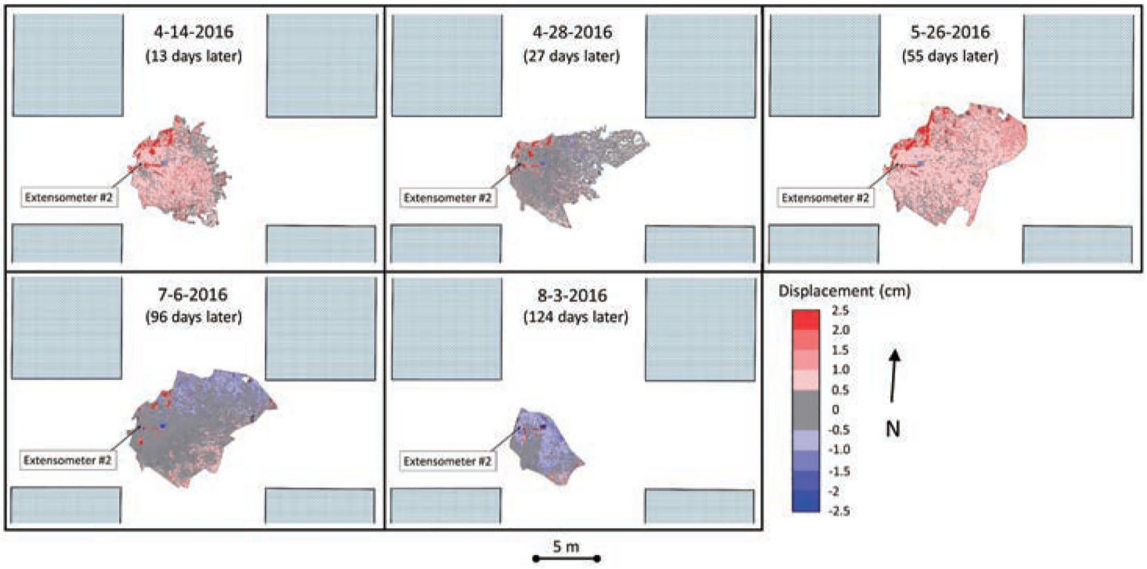

Figure 7 -

Floor movement according to the photogrammetric reconstruction at the extensometer #2 location.

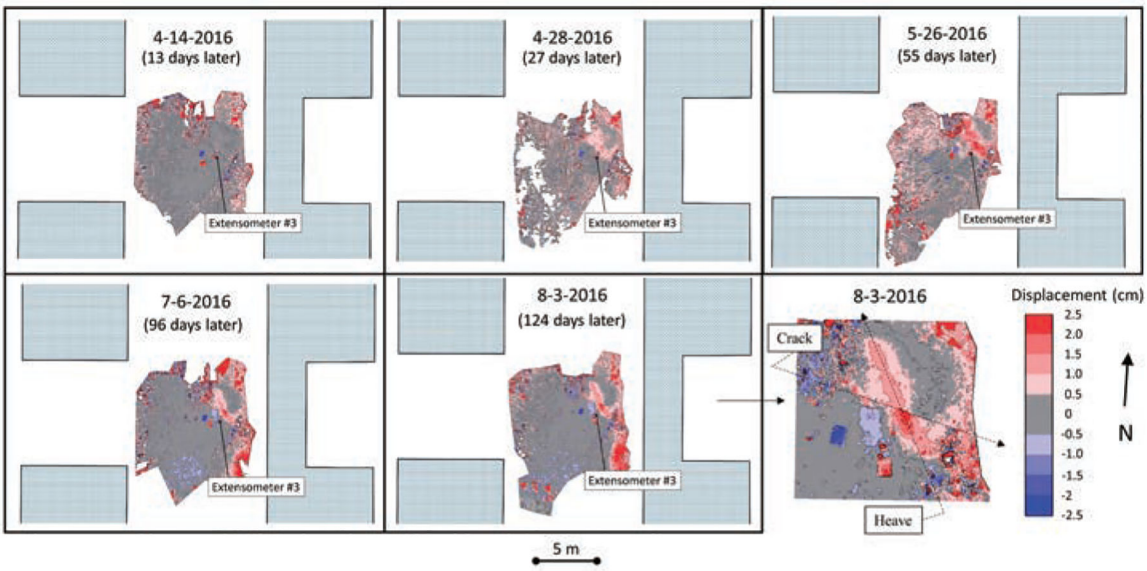

Figure 8 -

Floor movement according to the photogrammetric reconstruction at the extensometer #3 location.

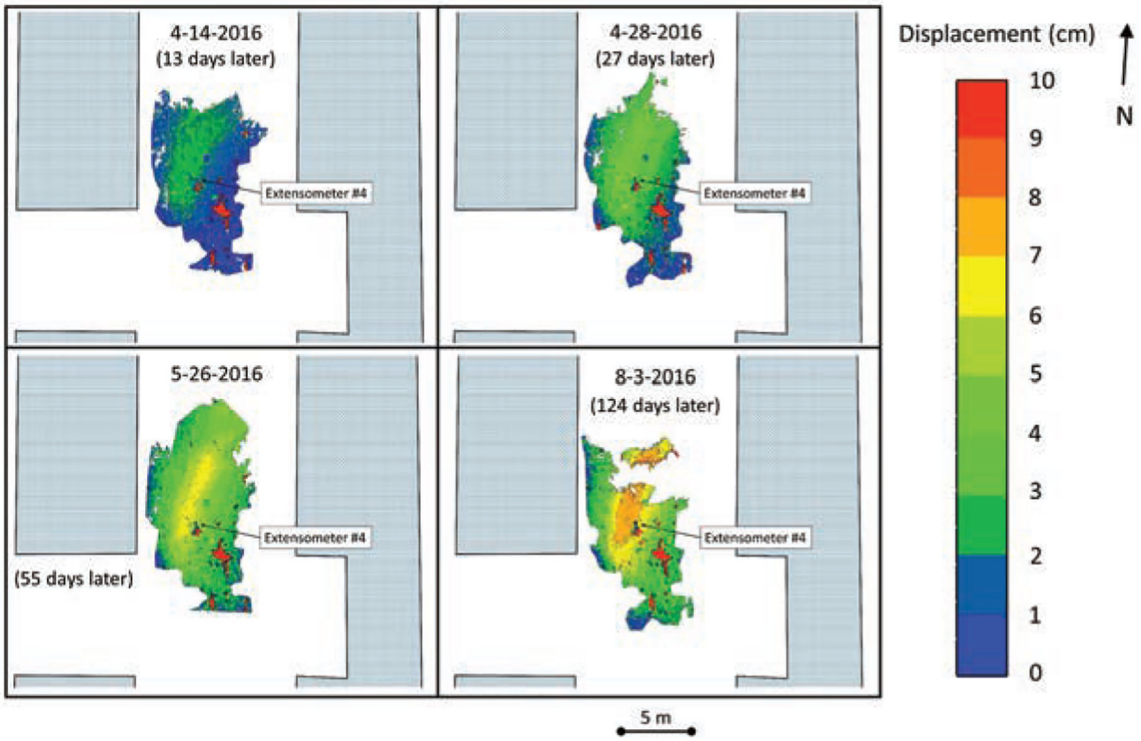

Figure 9 -

Absolute floor movement according to the photogrammetric reconstruction at the extensometer #4 location.

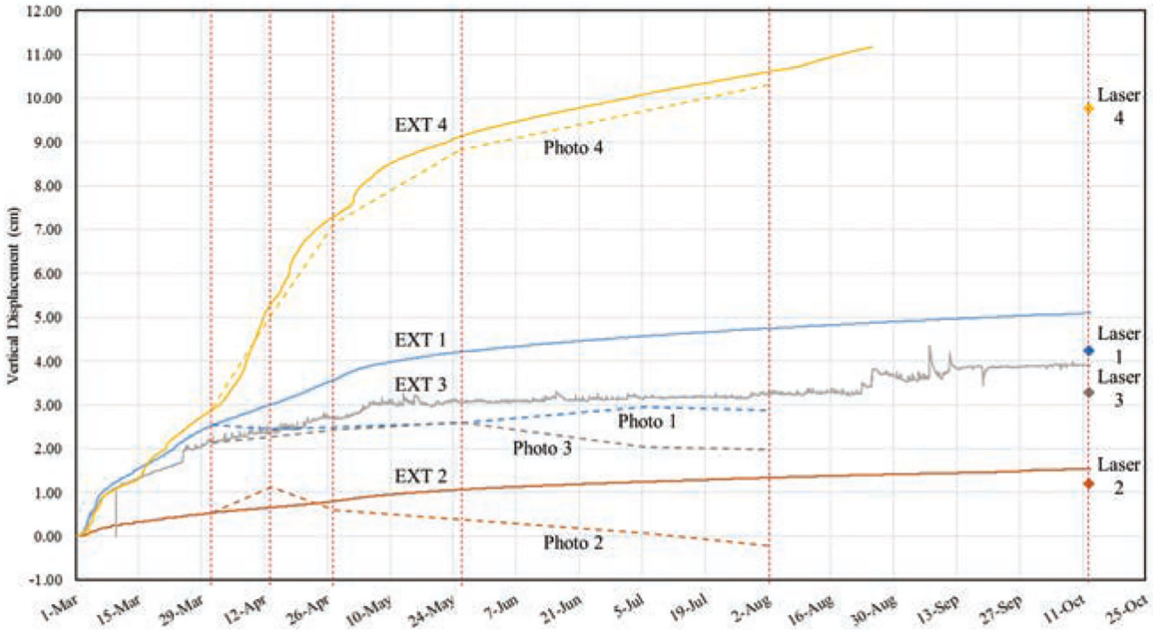

Figure 10 -

Extensometer and photogrammetry vertical displacement measurements on the floor at the four study sites. Dotted red lines represent the trips that were made to perform photogrammetry or laser surveys.

Data are labeled above (extensometer) and below (photogrammetry) their respective line. The laser measurements were only performed on Oct. 13.